Title

Reduction of Thrombosis and Bacterial Infection via Controlled Nitric Oxide (NO) Release from S-Nitroso-N-acetylpenicillamine (SNAP) Impregnated CarboSil Intravascular Catheters

Journal

ACS Biomaterials Science & Engineering, 3(3)

ISSN

2373-9878

Authors

Wo, Yaqi
Brisbois, Elizabeth J
Wu, Jianfeng
et al.

Publication Date

2017-03-13

DOI

10.1021/acsbiomaterials.6b00622

ACS Biomaterials SCIENCE & ENGINEERING

Article

pubs.acs.org/journal/abseba

Reduction of Thrombosis and Bacterial Infection via Controlled Nitric Oxide (NO) Release from *S*-Nitroso-*N*-acetylpenicillamine (SNAP) Impregnated CarboSil Intravascular Catheters

Yaqi Wo,[†] Elizabeth J. Brisbois,[‡] Jianfeng Wu,[§] Zi Li,[†] Terry C. Major,[‡] Azmath Mohammed,[‡] Xianglong Wang,[∥] Alessandro Colletta,[†] Joseph L. Bull,[∥] Adam J. Matzger,[†] Chuanwu Xi,[§] Robert H. Bartlett,[‡] and Mark E. Meyerhoff*[,†]

[†]Department of Chemistry, [‡]Department of Surgery, University of Michigan Medical Center, [§]Department of Environmental Health Sciences, and [∥]Department of Biomedical Engineering, University of Michigan, Ann Arbor, Michigan 48109, United States

Supporting Information

ABSTRACT: Nitric oxide (NO) has many important physiological functions, including its ability to inhibit platelet activation and serve as potent antimicrobial agent. The multiple roles of NO in vivo have led to great interest in the development of biomaterials that can deliver NO for specific biomedical applications. Herein, we report a simple solvent impregnation technique to incorporate a nontoxic NO donor, *S*-nitroso-*N*-acetylpenicillamine (SNAP), into a more biocompatible biomedical grade polymer, CarboSil 20 80A. The resulting polymer-crystal composite material yields a very stable, long-term NO release biomaterial. The SNAP impregnation process is carefully characterized and optimized, and it is shown that SNAP crystal formation occurs in the bulk of the polymer after solvent evaporation. LC-MS results demonstrate that more than 70% of NO release from this new composite material originates from the SNAP embedded CarboSil phase, and not from the SNAP species leaching out into the soaking solution. Catheters prepared with CarboSil and then impregnated with 15 wt % SNAP provide a controlled NO release over a 14 d period at physiologically relevant fluxes and are shown to significantly reduce long-term (14 day) bacterial biofilm formation against *Staphylococcus epidermidis* and *Pseudonomas aeruginosa* in a CDC bioreactor model. After 7 h of catheter implantation in the jugular veins of rabbit, the SNAP CarboSil catheters exhibit a 96% reduction in thrombus area (0.03 ± 0.01 cm^2/catheter) compared to the controls (0.84 ± 0.19 cm^2/catheter) (n = 3). These results suggest that SNAP impregnated CarboSil can become an attractive new biomaterial for use in preparing intravascular catheters and other implanted medical devices.

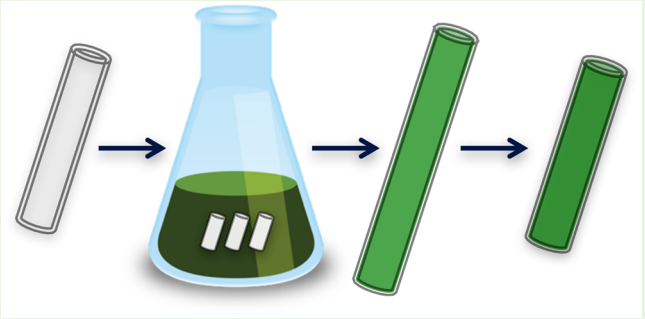

KEYWORDS: *nitric oxide, S-nitroso-N-acetylpenicillamine (SNAP), solvent impregnation, thromboresistance, bactericidal, antimicrobial catheters*

1. INTRODUCTION

Intravascular (IV) catheters are indispensable in modern-day medical practice, especially within hospital intensive care units.[1,2] They provide the necessary vascular access that allows doctors to withdraw blood samples, monitor patients, and administer medicine in a simple fashion; however, their frequent and prolonged use increase patients' risk for complications such as thrombosis and local or systemic infections.[3] Catheter-related thrombosis (CRT) is a common complication in patients with long-term indwelling catheters,[4] and it becomes symptomatic in about 5% of the patients.[5] Device-initiated thrombus formation can lead to thrombi detachment from the device surface that can travel through the vasculature and cause life-threatening obstructions such as pulmonary embolism, deep vein thrombosis, stroke or heart attack.[2,5,6] Use of systemic anticoagulants to prevent CRT is common, but not always effective,[5] and can increase the risk of causing hemorrhage[7,8] and/or inducing thrombocytopenia.[7]

Another major complication associated with IV catheter placement is infection.[1,9−11] Bacterial biofilm, commonly formed on surfaces by microbes sticking to each other, are surrounded and protected by a self-produced extracellular polymeric matrix. The presence of biofilm is one of the main causes of catheter-related bloodstream infections (CRBSIs).[3,11,12] Bacterial cells within biofilm are significantly more resistant to antibiotics as well as the patient's innate immune defense system than planktonic phase microbes, and the minimal concentration of antibiotics for eradication of mature biofilm is typically 10−1000 times higher than for the

Received: October 11, 2016
Accepted: January 21, 2017
Published: January 22, 2017

DOI: 10.1021/acsbiomaterials.6b00622
ACS Biomater. Sci. Eng. 2017, 3, 349−359

planktonic cells.[13,14] CRBSIs are the most common cause of nosocomial bacteremia,[10] and each year 150 million IV catheters are implanted in the United States,[15,16] and 250 000 CRBSIs occur annually because of their use.[9,16,17] As a result, it has been reported that CRBSIs dramatically increase the length of hospital stays,[18] mortality rates,[19] and overall treatment cost[9,20] per episode.

Many strategies have been suggested in the past to prevent thrombosis and infections from occurring on IV catheters, such as using a catheter lock solution that contains anticoagulant (e.g., heparin) and/or high concentration of antimicrobial agents (e.g., antibiotics).[7,21] Although there has been some success in clinical trials using these methods,[21] others have reported no significant differences in thrombosis reduction when using a heparin lock solution vs saline solution.[7,22,23] And for most of the studies evaluating antimicrobial lock solutions, the treatment was only evaluated based on negative blood sample cultures, not the presence or absence of biofilm on the catheter itself, a much more specific infection risk indicator.[11] Moreover, there are many concerns emerging from the potential toxicity to the patient resulting from the diffusion or inadvertent flushing of the lock solution into blood circulation,[11,24] as well as the development of antimicrobial resistance.[11,25]

Nitric oxide (NO) is synthesized in the human body from the substrate L-arginine[26] and participates in a variety of physiological processes, including vasodilation, blood pressure regulation, inhibiting platelet activation, maintaining hemostasis in the vasculature, immune response, and wound healing.[27−30] Nitric oxide can prevent activation of platelets, a key step in the coagulation cascade that ultimately leads to thrombus formation.[29,31] Nitric oxide has also been shown to exhibit broad-spectrum antibacterial activity against both Gram-positive and Gram-negative bacteria, including methicillin-resistant *Staphylococcus aureus* (MRSA).[27,32] NO serves as a bactericidal agent at high levels (200 ppm of gaseous NO),[33−35] but low levels of NO (picomolar to nanomolar range in solution phase) are also a key signaling molecule and mediator in bacterial quorum sensing to minimize bacterial adhesion and disperse biofilm formation.[36,37] Various *S*-nitrosothiols (RSNOs) are leading candidates as NO donors for incorporation into biomaterials for controlled NO delivery, because of their relatively high stability and ability to release NO under physiological conditions.[38−40] *S*-Nitroso-*N*-acetylpenicillamine (SNAP) is a particularly attractive RSNO species for creating NO releasing biomedical devices because of its low cost, safety (e.g., penicillamine is an FDA-approved drug[41]), and potential for long-term NO release applications when it is incorporated into biomedical polymers with very low water uptake.[42,43]

Recently, our lab has developed a very simple impregnation procedure in which SNAP can be impregnated into commercial silicone rubber Foley urinary catheters to achieve long-term NO release capabilities (>30 days).[44] In this previous work, Colletta et al. obtained 5.43 wt % of SNAP-within the silicone Foley catheter by impregnating the tubing for 24 h in a 125 mg/mL SNAP solution prepared in THF. The antimicrobial efficiency of the NO releasing Foley catheters was demonstrated toward several strains of bacteria associated with catheter associated urinary tract infections. In follow-up work, Brisbois et al. reported the impregnation of commercial Tygon formula 3350 silicone tubing using 25 mg/mL of SNAP in THF for 24 h and then used the tubing for preparing extracorporeal circuits (ECC). These NO releasing ECC loops exhibited improved blood compatibility over corresponding controls without NO release in a 4 h rabbit thrombogenicity model.[45]

It is well-known that molecular interactions between polymer surfaces and protein molecules determine the biocompatibility of a polymer[46] and the innate hemocompatibility of the polymer that contacts blood can greatly influence its ultimate efficacy in preventing thrombus formation.[47] Indeed, Handa et al. evaluated the intrinsic hemocompatibility of four different biomedical grade polymers in vivo and the results demonstrated that polyurethane copolymers (such as Elast-eon E2As, a block copolymer of polyurethane and poly(dimethylsiloxane) have enhanced inherent hemocompatibility compared to the other polymers, including polyurethanes (e.g., Tecoflex SG-80A) and poly(vinyl chloride) (PVC).[47] CarboSil 20 80A, similar to Elast-eon E2As, is a triblock copolymer of polyurethane, poly(dimethylsiloxane) and polycarbonate, synthesized from hard segments 4,4′-methylene bisphenyl diisocyanate with glycol chain extender and soft segments of aliphatic polycarbonate and poly(dimethylsiloxane).[46] Studies have shown that there is a strong interaction between fibrinogen and the CarboSil polymer surface that results in very few conformational changes of the adsorbed fibrinogen, which is an important step in preventing the coagulation cascade and thrombus formation initiated by protein adsorption.[27] Therefore, CarboSil is a very attractive material for preparing IV catheters owing to its enhanced innate hemocompatibility.[43,46] IV catheters or other biomedical devices made with NO releasing CarboSil should have more enhanced efficacy in reducing platelet activation and thrombus formation than CarboSil alone. Of note, the impregnation method described earlier[44,45] was developed for silicone rubber and THF is a good solvent for silicone because it can swell the tubing to ca. 1.3 times its original size.[45] However, the compatibility between various solvents and polymers are quite different in different scenarios.[48] For example, since THF is known to be able to dissolve, instead of swell, CarboSil polymer,[43] different solvents need to be selected in order to adapt this methodology to CarboSil. Moreover, many other aspects of the previously reported impregnation process (e.g., the SNAP concentration, impregnation time, etc.) need to be optimized to achieve the best efficiency for SNAP impregnation into CarboSil. Herein, we report our effort to modify the SNAP impregnation method to transform premade dip-coated CarboSil 20 80A IV catheters into NO releasing catheters. The optimized SNAP impregnation process and material characterization (including solid-state analysis of the SNAP within the CarboSil polymer) are described in detail. The resulting catheters are further evaluated for their antimicrobial efficacies in vitro against *Staphylococcus epidermidis*[16,49,50] and *Pseudomonas aeruginosa*,[10] two bacteria that are commonly reported to cause CRBSIs. In addition, the IV CarboSil catheters are also evaluated within the jugular veins of rabbits to examine their effectiveness at preventing thrombus formation.

2. EXPERIMENTAL SECTION

2.1. Materials. *N*-Acetyl-D-penicillamine (NAP), sodium nitrite, L-cysteine, sodium chloride, potassium chloride, sodium phosphate dibasic, potassium phosphate monobasic, copper(II) chloride, ethylenediaminetetraacetic acid (EDTA), tetrahydrofuran (THF) and *N*,*N*-dimethylacetamide (DMAc) were purchased from Sigma-Aldrich (St. Louis, MO). *N*-Acetyl-D,L-penicillamine disulfide (NAP disulfide) was obtained from Enzo Life Science, Inc. (New York, NY). Methanol

DOI: 10.1021/acsbiomaterials.6b00622
ACS Biomater. Sci. Eng. 2017, 3, 349−359

(MeOH), methyl ethyl ketone (MEK), hydrochloric acid, sulfuric acid, Luria–Bertani (LB) broth and LB agar were products of Fisher Scientific (Hampton, NH). CarboSil 20 80A was obtained from DSM Biomedical Inc. (Berkeley, CA). An Agilent ZORBAX rapid resolution high definition (RRHD) Eclipse Plus C18 column (2.1 × 50 mm, 1.8 μm particle size) was purchased from Altmann Analytik GmbH & Co.KG (Munich, Germany). All aqueous solutions were prepared with 18.2 MΩ-deionized water using a Milli-Q filter from EMD Millipore (Billerica, MA). Phosphate buffered saline (PBS), pH 7.4, containing 138 mM NaCl, 2.7 mM KCl, 10 mM sodium phosphate, and 100 μM EDTA was used for all in vitro experiments. *S. epidermidis* ATCC 14990 and *P. aeruginosa* ATCC 27853 were obtained from the American Type Culture Collection (ATCC) (Manassas, VA).

2.2. Preparation of SNAP-Impregnated Films and Catheters. In order to determine the ideal solvent combination for optimal SNAP impregnation into CarboSil, a series of solvents were screened for their ability to swell CarboSil polymer pellets and dissolve SNAP. The swelling capability of the solvents was reported in percent as

$$\text{swelling ratio (\%)} = [(R_{\text{after}} - R_{\text{before}})/R_{\text{before}}] \times 100 \quad (1)$$

where R_{before} and R_{after} are the radius of the polymer pellets before and after the solvent impregnation process, respectively.

Polymer films containing various wt % of SNAP were prepared by solvent impregnation. First, 200 mg of the CarboSil polymer was dissolved in 2 mL THF and then cast in a Teflon ring (d = 2.5 cm) on a Teflon plate and left to dry overnight under ambient condition to obtain the blank polymer films. Small disks (d = 0.7 cm) were cut from the parent films and used as blank films. Some blank CarboSil films were impregnated in SNAP solutions (120 mg/mL) in 30% MeOH and 70% MEK for different lengths of time and the amount of SNAP (wt %) in the final films was analyzed to obtain time needed to achieve maximum SNAP impregnation into the polymer films. The CarboSil films were also treated with solutions containing different concentrations of SNAP (5.5–120 mg/mL) for 2 h to achieve a polymer impregnation profile in regard to the SNAP concentration in the impregnation solution.

The catheters used in the in vitro and in vivo experiments were prepared by dip coating CarboSil polymer solution on 20 cm long stainless steel mandrels of 1.0 mm diameter (McMaster Carr, IL). The control catheters and SNAP catheters were preparing by dip coating 22 coats and 20 coats of polymer solution at 2 min intervals between each coat, respectively. All catheters were allowed to dry overnight under ambient conditions, protected from light, and then removed from the mandrel. Similar to the SNAP-impregnated films, the SNAP-doped catheters were also prepared by soaking in a SNAP solution (120 mg/mL) for 2 h. The catheters were removed from the solution, rinsed with MeOH to wash off the residual SNAP solution on the surfaces, and then allowed to air-dry overnight to allow the MeOH and MEK solvents to evaporate further, while the SNAP remains in the catheter. To achieve a smoother surface after impregnation and to prolong NO release, two coats of plain CarboSil polymer solution were applied to the outer surface of the SNAP-impregnated catheters by dip-coating to achieve a total of 22 coats. All the cured films and catheters were dried under vacuum for an additional 48 h to remove solvents more thoroughly. The resulting catheters have an i.d. of 1 mm and an o.d. of 2.2 mm.

2.3. Characterization of SNAP-Impregnated Films and Catheters. *2.3.1. UV–vis.* All UV–vis spectra of solvent dissolved pieces of known mass of the films or catheters (in DMAc) were recorded in the wavelength range of 250–650 nm with a UV–vis spectrophotometer (Lambda 35, PerkinElmer, MA) at room temperature. The molar absorptivity of SNAP in PBS at 340 nm was determined as $\varepsilon_{\text{SNAP}}$= 1075 M^{-1} cm^{-1}. The characteristic absorbance at 340 and 590 nm correlate to the $\pi \rightarrow \pi^*$ and $n_N \rightarrow \pi^*$ electronic transitions of the S-NO functional group.[51,52]

2.3.2. NO Release Measurement from SNAP-Impregnated Catheters. Nitric oxide release from the SNAP-impregnated CarboSil catheters was measured using a Sievers chemiluminescence Nitric Oxide Analyzer (NOA) 280i (Boulder, CO). For example, a 15 wt % SNAP-impregnated CarboSil catheter with 2 CarboSil topcoats was placed in the sample vial containing 4 mL of 10 mM PBS, pH 7.4, with 100 μM EDTA at 37 °C to mimic physiological conditions. Nitric oxide was continuously generated and immediately purged and swept into the chemiluminescence detection chamber by a N_2 sweep gas and bubbler. All catheters were placed in fresh PBS buffer during NO release measurements and incubated at 37 °C in the absence of ambient light after each measurement. The reported NO flux was the average flux during 4 h of NO release measurements for each time point.

2.3.3. Cumulative NAP, NAP Disulfide, and SNAP Leaching from SNAP-Impregnated Catheters in Soaking PBS Buffer. The cumulative leaching of NAP, NAP disulfide and SNAP from the impregnated catheters into 10 mM PBS, pH 7.4, with 100 μM EDTA at 37 °C were analyzed using liquid chromatography-tandem mass spectrometry (LC-MS), as previously described in detail.[43] Briefly, 15 wt % SNAP-impregnated CarboSil catheters were incubated in 10 mL PBS buffer, pH 7.4, with 100 μM EDTA (to minimize trace metal catalyzed decomposition of SNAP) in the dark at 37 °C to minimize trace metal catalyzed decomposition of SNAP. At various time points, aliquots (15 μL) of the soaking solution were analyzed for the amount of NAP, NAP disulfide and SNAP in the soaking buffer. The total amount of SNAP-related species is calculated from the following equation

$$[\text{all SNAP-related species}]_{\text{total}} = [\text{SNAP}]_{\text{total}} + [\text{NAP}]_{\text{total}} + 2[\text{NAP disulfide}]_{\text{total}} \quad (2)$$

The soaking buffer was replaced with new buffer immediately after the measurement. The total amount of NAP, SNAP and SNAP disulfide leached from the catheter was determined over 14 consecutive days of measurements.

2.3.4. Evaluation of the Mechanical Properties for Catheters before and after Impregnation. Four different catheters (5 cm) were prepared for mechanical property tests, including the original CarboSil catheters prepared by dipcoating, CarboSil catheters swelled by solvents only (and then dried), CarboSil catheters impregnated with 7 and 15 wt % SNAP, respectively. Tensile testing of the catheters was performed on an Instron 8800-series machine with Bluehill software (Instron, Norwood, MA). To achieve a better grip on the catheters, the catheters were cut in halves along the axial direction before testing. The catheters had an initial gauge length of 11.55 mm and were pulled at an extension rate of 40 mm/min, corresponding to a strain rate of 0.0593 s^{-1}. The tensile strength (MPa) and maximum elongation (elongated length over the length of the original) were compared for each of the catheter materials tested.

2.4. Long-Term (14 days) in Vitro Antibacterial Experiments. *S. epidermidis* (ATCC 14990) and *P. aeruginosa* (ATCC 27853) were used as model bacterial strains in this study. Biofilm was developed onto the surfaces of both control and NO release CarboSil catheters for 14 d using a CDC biofilm reactor (Biosurface Technologies Corp., Bozeman, MT). Details of the microbiology procedures used in relation to these studies reported are provided in the Supporting Information.

2.5. in Vivo Antithrombotic Evaluation of Intravascular Catheter in Rabbit Model. All animal handling and surgical procedures employed in this research were approved by the University of Michigan Committee on the Use and Care of Animals in accordance with university and federal regulations. In short, 5 cm lengths of the catheters (one SNAP-impregnated and one control) were inserted into the external jugular veins of rabbits for 7 h to test the hemocompability of both types of catheters. The detailed animal experiment procedures are provided in the Supporting Information. At the end of the 7 h of experiments, the catheters were carefully explanted from the veins with the thrombus intact on the catheter surface. ImageJ imaging software provided by the National Institutes of Health (NIH) was used to quantify the thrombus area on the surface of both types of catheters.

2.6. Statistical Analysis. All experiments were conducted in triplicate. Data are all expressed as mean ± SEM (standard error of the mean). Comparison of means using student's t test was utilized to analyze the statistical differences between SNAP-impregnated

DOI: 10.1021/acsbiomaterials.6b00622
ACS Biomater. Sci. Eng. 2017, 3, 349–359

catheters and control catheters. Values of $p < 0.05$ were considered statistically significant for all tests.

3. RESULTS AND DISCUSSION

3.1. Study of SNAP Impregnation Process of CarboSil Polymer Films. To achieve desired SNAP loading into the CarboSil polymer, an ideal solvent or solvent mixture needs to be employed that has the following properties: (1) high solubility of SNAP; (2) ability to significantly swell CarboSil polymer without harming the material; and (3) evaporate to dryness in a reasonable time period. Therefore, a series of solvents were examined for their ability to swell the CarboSil polymer pellets as well as their SNAP solubility limit. The swell ratio ($[(R_{after} - R_{before})/R_{before}] \times 100$) of solvents were compared and methyl ethyl ketone (MEK) was found to exhibit the highest swell ratio of 166 ± 9% (with 155 ± 4% for acetone, 135 ± 3% for ethyl acetate and 110 ± 3% for methanol (MeOH)). However, solubility tests indicated that the SNAP solubility is only 30 mg/mL in MEK, 70 mg/mL in acetone, and 30 mg/mL in ethyl acetate, but 330 mg/mL in MeOH. As a result, a combination of MEK and MeOH was studied in order to determine the optimal solvent composition for maximized SNAP impregnation into CarboSil films and catheters, without destroying the structure of polymer.

To optimize the MEK/MeOH solvent mixture for impregnation, we totally immersed CarboSil polymeric materials (pellets, films or catheters) into various MEK/MeOH swelling solutions. Then, the material was removed from the swelling chamber, quickly rinsed with MeOH and DI water to decrease any residue on the surface, and then air-dried in the ambient environment protected from light exposure. After this process, the polymer material was weighed, and then the impregnated polymer was dissolved in DMAc for UV−vis absorbance measurements to determine the total amount of SNAP incorporated into the final CarboSil material. The results shown in Figure 1 demonstrate that the optimal solvent

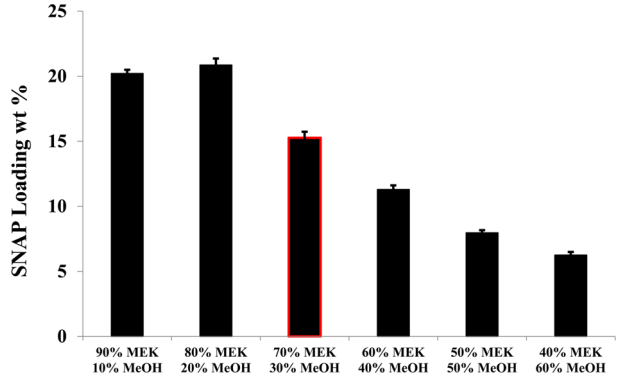

Figure 1. Weight percentage (wt %) of SNAP achieved in CarboSil pellets (mg SNAP/mg impregnated CarboSil pellet ×100%) using different solvent mixtures for the impregnation process.

combination is 70% MEK and 30% MeOH (volume ratio). However, 90% MEK, 10% MeOH and 80% MEK, 20% MeOH can technically incorporate more total SNAP into the CarboSil polymer, but the polymer pellets were easily destroyed and cracked apart during the drying process using these ratios of solvents. As shown in Figure S2, the amount of SNAP impregnated into CarboSil can be modulated and the level directly correlates with the concentration of SNAP employed in the swelling solution (70% MEK and 30% MeOH). Indeed, the wt % of SNAP in the final CarboSil material increased from 2.5 to 15.7% in near linear fashion when the SNAP concentration increased from 5.5 to 120 mg/mL.

To study the SNAP impregnation kinetics as a function of polymer film thickness and to determine the time required to achieve maximum impregnation, blank CarboSil films of both 250 and 500 μm in thickness were prepared. The films were then soaked into a solution of 120 mg/mL SNAP in 70% MEK/30% MeOH ($n = 3$ for each condition), for 1, 2, 3, 5, 10, 30, 60, 90, 120, and 150 min, respectively. After thorough drying, the films were weighed and then dissolved in DMAc to quantify the SNAP wt % within the films. The impregnation profile (Figure 2) indicated that the maximum impregnation is

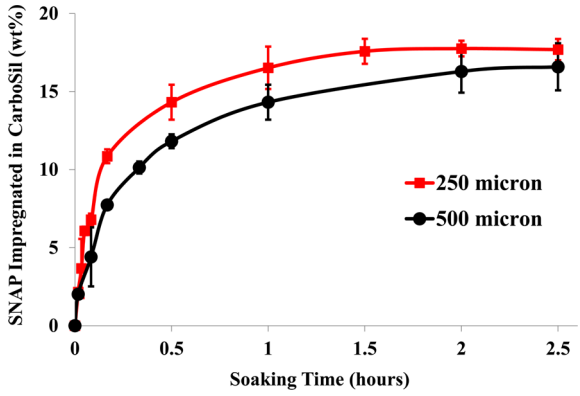

Figure 2. Kinetics of SNAP impregnation in CarboSil film using 120 mg/mL SNAP in swelling solution (70% MEK and 30% MeOH), with respect to swelling time and polymer thickness. The results indicate that maximum SNAP incorporation is achieved within 2 h of swelling and there is no significant difference in loading when using films with different thickness (250 μm vs 500 μm).

achieved within 2 h, and there is no significant difference between 250 μm thick films and 500 μm thick films. This suggests that the solvent impregnation process is capable of incorporating SNAP into various sized catheters (different wall thicknesses, etc.) without requiring any significant additional time for the impregnation process.

3.2. Solid-State Analysis of SNAP-Impregnated CarboSil Polymer System. Our group has previously reported solid-state studies of SNAP-doped CarboSil films formed by casting a THF solution containing SNAP and CarboSil polymer into a Teflon plate and allowing the solvent to completely evaporate.[43] The elevated shelf life stability of SNAP in CarboSil was only observed when the SNAP level within the CarboSil exceeds its solubility in the CarboSil and forms orthorhombic crystals that embed in the bulk of the polymer matrix. In this work that demonstrates the SNAP impregnation approach using premade CarboSil films, similar solid-state characterizations were conducted to examine the resulting films. As shown in Figure S3), clear SNAP crystalline patterns were observed for the 5 wt % SNAP-impregnated samples under a polarized microscope, indicating to the presence of SNAP crystals in the polymer matrix at this SNAP concentration. Additional microscope images of the cross-section of the SNAP-impregnated CarboSil films were also taken to determine if SNAP impregnated into the bulk polymer matrix or if the crystals exhibit depth dependent distribution when they are formed after the solvent evaporates. Thin slices (30 μm) of the cross-section of 5 wt % SNAP-impregnated

DOI: 10.1021/acsbiomaterials.6b00622
ACS Biomater. Sci. Eng. 2017, 3, 349−359

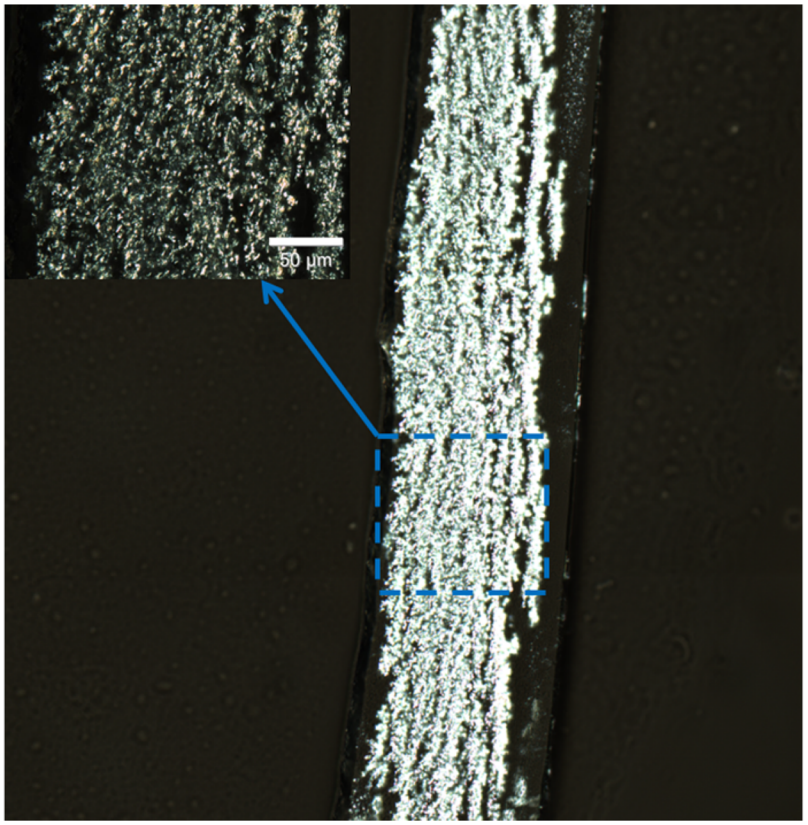

Figure 3. Representative optical images of the cross-section of 5 wt % SNAP-impregnated CarboSil films. The images were captured by Leica DM2500 LED microscope with a 20× and a 50× (inset) objective under crossed polarizers. The cross-section of film samples was cut into 30 μm thick slices by the Leica 3050S cryostat. The SNAP was impregnated successfully into the bulk of the polymer film and distributed relatively evenly throughout the cross-section.

CarboSil films were obtained by using the Leica 3050S cryostat. Figure 3 shows examples of the optical images of the cross section of the film, which clearly illustrate that SNAP crystals are distributed relatively uniformly within the polymer matrix after impregnation, rather than merely present on the polymer film's outer surfaces.

In principle, SNAP's solubility limit in the CarboSil polymer should be constant regardless of preparation methodology (e.g., casting polymer solution or solvent impregnation). The PXRD patterns of the CarboSil films impregnated with various loading of SNAP were collected and analyzed (Figure 4). In our previous work, the solubility of SNAP in CarboSil when SNAP was added into polymer solution before casting was calculated by using the ratio of a selected SNAP crystalline peak area over the total area of the sample pattern.[43] Herein the method used to calculate the SNAP solubility in the polymers used the ratio of peak heights instead of peak area because this is more generally applicable to various polymers that have broad diffraction peaks. In short, based on the following assumptions that (1) crystalline SNAP is uniformly distributed in the polymer phase, and (2) that the preferred orientation of SNAP crystals in the polymer could be eliminated by cutting samples into cubes and rotating the samples during data collection, the ratio of a specific SNAP crystalline peak height over the polymer peak height should be proportional to the ratio of crystalline SNAP wt % over the polymer wt % in the sample. By using the height ratio for quantification, all of the other factors that can potentially influence peak intensity (e.g., the volume of the sample irradiated by the X-ray source, the exposure time of sample under the X-ray, etc.) can be eliminated. Here, the SNAP solubility in polymer, represented as x_o, can be calculated from $y_{2\theta}$, the height ratio of a SNAP peak over the height of a polymer peak

$$y_{2\theta} = \frac{I_{\mathrm{SNAP}2\theta}}{I_{\mathrm{polymer}2\theta}} = \frac{a(x - x_o)}{b(1 - x)} \tag{3}$$

where $I_{\mathrm{SNAP}2\theta}$ and Ipolymer$_{2\theta}$ are the signal intensities of SNAP and polymer in a SNAP impregnated polymer sample at angle 2θ, obtained in each measurement. For a PXRD pattern of a unit volume sample taken with a unit exposure time, a and b correspond to the peak height of pure orthorhombic crystal and blank CarboSil pattern at a given 2θ, respectively. When the SNAP weight percentage is x, the height ratio of SNAP peak height over CarboSil peak height at a given 2θ ($y_{2\theta}$), should be proportional to the weight percentage ratio of the undissolved SNAP crystal ($x - x_o$) over the weight percentage of CarboSil ($1-x$). By substituting various x and $y_{2\theta}$ at chosen 2θ angles, the solubility x_o can be determined. Based on this calculation, the solubility of SNAP in the impregnated CarboSil material was found to be 2.4 ± 0.1 wt %, which is significantly lower than the result of 4.3 ± 0.3 wt %, calculated from films obtained by casting SNAP and CarboSil polymer solution (if also using this height based method).[43]

We attribute the decrease in calculated SNAP solubility to insufficient "dissolution" of impregnated SNAP molecules in the polymer to reach its solubility equilibrium in the polymer phase during the solvent impregnation method. When the polymer film is prepared by casting dissolved SNAP in a

DOI: 10.1021/acsbiomaterials.6b00622
ACS Biomater. Sci. Eng. 2017, 3, 349−359

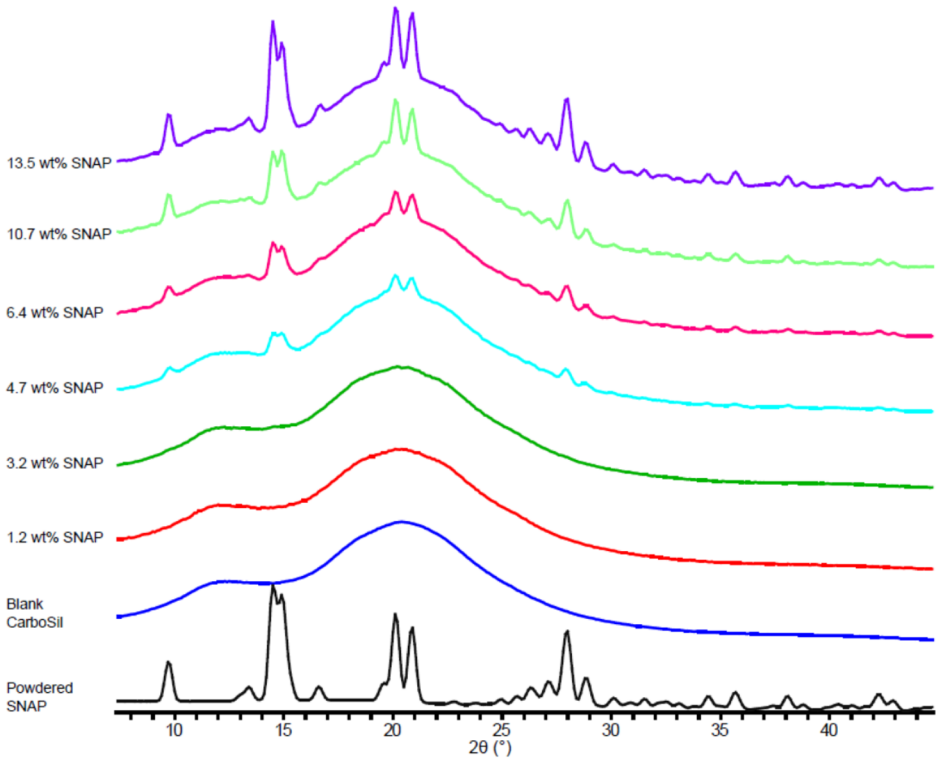

Figure 4. Representative PXRD patterns of orthorhombic SNAP crystal, CarboSil blank polymer, and CarboSil impregnated with SNAP of different weight percentages. Characteristic peaks of orthorhombic SNAP were detected in samples. Peak intensity of crystalline SNAP increased with higher loading of SNAP in polymer.

CarboSil solution (in THF),[43] the SNAP molecules and CarboSil polymer chains are uniformly mixed within the solvent. Therefore, the SNAP molecules are well dispersed in the polymer matrix to form a solid polymer solution before the solvent completely evaporates and the solution reaches its SNAP solubility limit which ultimately leads to the SNAP crystallization (Figure S4A). However, during the swelling-impregnation process, SNAP can only be "inserted" into the space between polymer chains when the premade CarboSil film is swelled by the MEK/MeOH solvent mixture. The diffusion of SNAP molecules within solid polymers may be less efficient compared to the polymer casting method when SNAP and polymer are all completely dissolved and well mixed. In addition, the swelling effect of solvent mixture may also vary for different polymer segments. For example, the interspace between the soft segments of CarboSil may be swelled more by the solvent and enable easier impregnation of SNAP molecules, which may result in different microenvironments for SNAP crystallization at the different polymer segment sites (see Figure S4B). In summary, we hypothesize that SNAP cannot diffuse and reach solubility equilibrium in the polymer during solvent impregnation as easily as it does when SNAP and polymer are well mixed in a solvent, as is in the polymer casting method. Therefore, SNAP aggregates as crystals and forms a polymer crystal composite more readily in the solvent impregnation process that uses premade polymer devices (e.g., films or catheters).

3.3. Mechanical Properties Tests. Tension testing was performed in order to assess the changes in mechanical properties caused by solvent swelling and SNAP impregnation. Of note, the Instron machine was not able to obtain a firm grip on the original CarboSil catheters during the elongation process with the current experimental setup. Thus, the analysis results below only contain three experimental groups; the swelling solvent only, 7 wt % SNAP, and 15 wt % SNAP, with triplicates of each type of sample tested ($n = 3$). One-way ANOVA results revealed no significant difference in tensile strength ($p = 0.15$) or maximum elongation ($p = 0.42$) among the three groups (see Figure 5). The results indicate that the catheters are still mechanically suitable for biomedical use after the impregnation process.

3.4. NO Release Measurement of SNAP-Impregnated CarboSil Catheters. The 15 wt % SNAP-impregnated CarboSil catheters with CarboSil topcoats release NO above a flux rate of 0.5×10^{-10} mol cm^{-2} min^{-1} for 14 d in PBS buffer at 37 °C. The NO release rate from the catheters was quantitated and recorded by chemiluminescence measurements. A burst of NO release ($\sim 4 \times 10^{-10}$ mol cm^{-2} min^{-1}) was observed on day 0, and this correlates with rapid SNAP leaching from the outermost layer of the catheter surface into the buffer. After depletion of the SNAP reservoir in this outermost region, the NO release rate drops to its minimal level at day 2 ($\sim 1 \times 10^{-10}$ mol cm^{-2} min^{-1}) and then gradually increases to 4×10^{-10} mol cm^{-2} min^{-1} over the next 10 d period (Figure 6). The NO release levels then drop below 0.5×10^{-10} mol cm^{-2} min^{-1} after d 14, as all the SNAP in the bulk of the polymer has decomposed. As indicated in Section 3.2 above, the majority of the SNAP molecules impregnated in the catheters are in their crystalline form, and it takes time for the crystalline SNAP embedded in the bulk of the polymer to dissolve and release its NO. We believe that this slow crystal dissolution process is the reason for the long-term NO release observed from these new SNAP-impregnated CarboSil catheters.

DOI: 10.1021/acsbiomaterials.6b00622
ACS Biomater. Sci. Eng. 2017, 3, 349−359

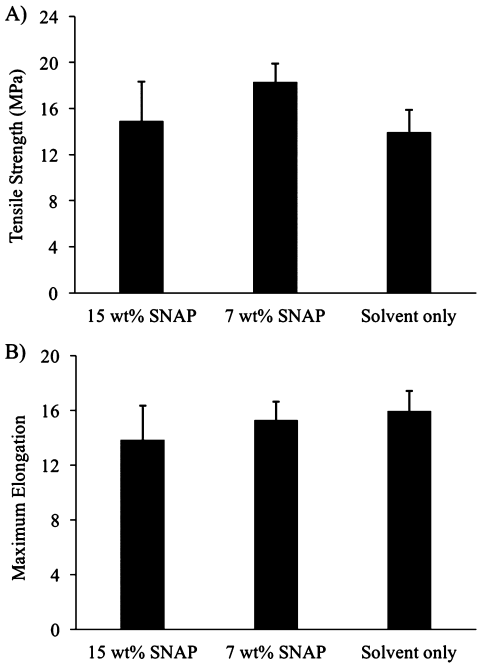

Figure 5. (A) Tensile strength testing and (B) the maximum elongation results for CarboSil tubing impregnated by solvents only, and CarboSil tubing with 7 and 15 wt % SNAP loading, respectively. Results are average ± SEM for n = 3 for each experiment.

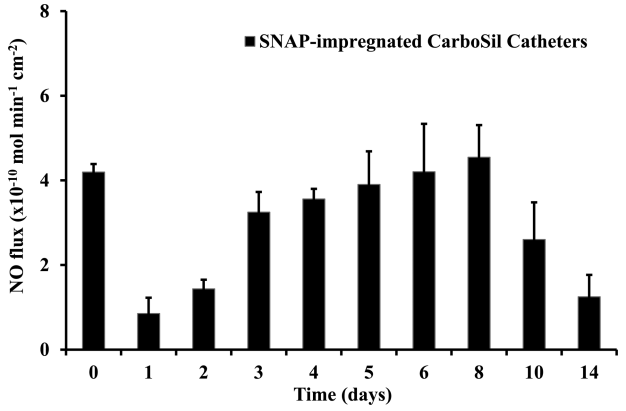

Figure 6. NO release profile of 15 wt % SNAP-impregnated CarboSil catheters over time. The catheters were prepared with CarboSil outer coating (n = 3).

3.5. Cumulative Leaching of NAP, NAP Disulfide, and SNAP from SNAP-Impregnated CarboSil Catheters. The concentrations of NAP, NAP disulfide and SNAP leached from SNAP-impregnated CarboSil catheters were monitored by LC-MS using a method previously reported.[43] As shown in Figure 7, 12% of the initial SNAP (80 nmol/mg polymer) diffuses out of the catheter over the 14 d test period. The rate of SNAP leaching is the greatest in the first few hours after introducing the catheter to the soaking buffer, and then a significant lower amount of SNAP continues to diffuse into the buffer over the following days. Similar leaching patterns were observed for both NAP and NAP disulfide. A total of 12 nmol/mg polymer NAP and 46 nmol/mg polymer NAP disulfide (2 and 14% of the initial SNAP present in the catheter, respectively) leached into the buffer over 2 weeks. NAP is the parent thiol used in SNAP synthesis, and NAP has been a widely used chelating and detoxifying agent for treating patients with heavy metal ion

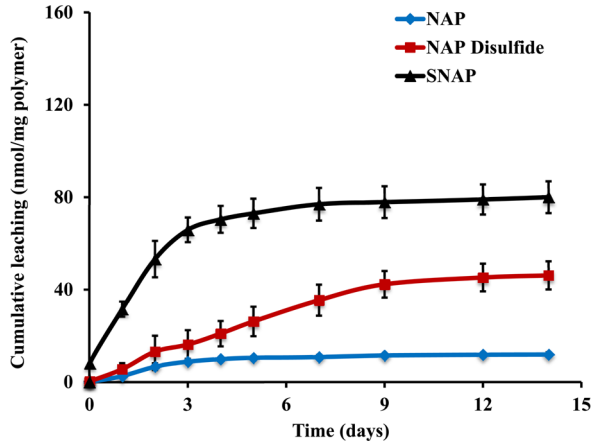

Figure 7. Cumulative leaching of NAP, NAP disulfide, and SNAP into 1 mL of PBS (soaking buffer) from 15 wt % SNAP-impregnated CarboSil catheters over a period of 14 days, at 37 °C in the dark. Data are mean ± SEM (n = 3).

poisoning (e.g., cadmium, arsenic, and mercury) for many years.[53,54] Therefore, NAP and NAP dimer (NAP disulfide) emitted from the SNAP catheter into the buffer or bloodstream are considered relatively safe and unlikely to cause any adverse or toxic response in potential clinical applications.[43] Overall, the total moles of SNAP-related species ($[\text{all SNAP-related species}]_{\text{total}}$) leached out over the 14 d test period is approximately 28% of the total NO (in moles) released from the catheter, which means more than 70% of the NO is released directly from SNAP molecules residing within polymeric matrix. Since NO is highly reactive in vivo and will be rapidly scavenged by surrounding species (e.g., oxyhemoglobin, oxygen),[55,56] to achieve therapeutic functions of NO, it is essential for the catheters to deliver localized NO release at their surface with minimal NO donor leaching. On the basis of results from the leaching studies, this appears to be the case for the new SNAP impregnated CarboSil biomaterial.

3.6. Prevention of Mature Microbial Biofilm Formation. Because stable NO release from biomedical devices is expected to reduce bacterial adhesion and proliferation, in vitro antimicrobial experiments were conducted to evaluate the efficacy of SNAP-impregnated Carbosil catheters against bacterial infections caused by microbes, *S. epidermidis* and *P. aeruginosa*, commonly responsible for catheter-related blood-stream infections. *S. epidermidis* has always been regarded as an innocuous and commensal inhabitant of healthy mucosal microflora and possesses lower pathogenic potential than *S. aureus* and *P. aeruginosa*,[57] but more recently *S. epidermidis* has been shown to be the most frequent cause of infections on indwelling medical devices.[50,58] This likely stems from the prevalence of *S. epidermidis* on human skin which results in a high probability of contamination during IV catheter insertion. It has also been reported that the primary virulence factor of *S. epidermidis* is its potential capability to form high-biomass biofilm.[44,59−61] Moreover, many studies have shown that treatment of *S. epidermidis* biofilm cells with high dose of antibiotics (e.g., rifampicin, vancomycin, etc.) accelerates the emergence of highly resistant cells.[16,62,63] Indeed, genome sequence studies of *S. epidermidis* strains isolated from IV catheters in the hospital have expressed specific antibiotic resistance genes and required much higher concentrations of antibiotics for treatment.[50,58,63,64] The cost related to CRBSIs

DOI: 10.1021/acsbiomaterials.6b00622
ACS Biomater. Sci. Eng. 2017, 3, 349−359

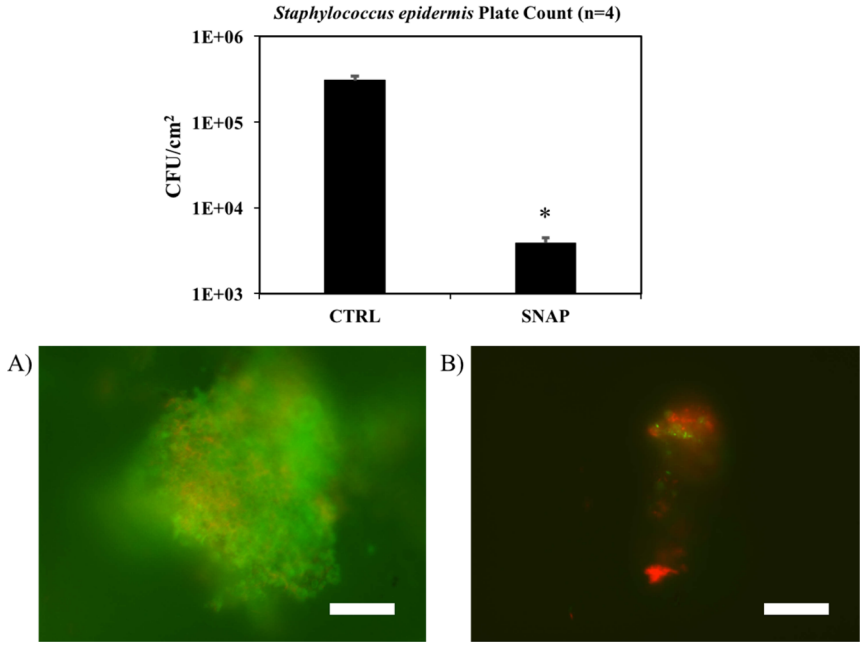

Figure 8. *S. epidermidis* biofilms developed on catheter segments in a CDC biofilm reactor for 14 d at 37 °C. Upper image: Bar graph of plate count data for adhesion of viable *S. epidermidis* bacteria to the catheter surfaces. Lower images: Representative fluorescence microscopic images of (A) surface live (green) and (B) dead (red) bacteria on different catheters, acquired by oil immersion 60× objective lens of the biofilms on the surface of the catheter, scale bar 20 μm.

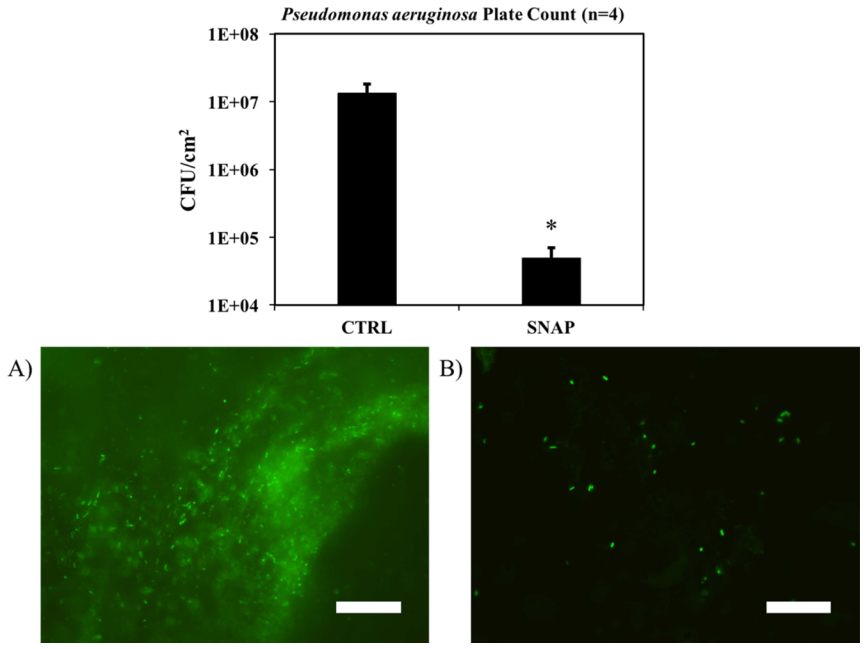

Figure 9. *P. aeruginosa* biofilms developed on catheter segments in a CDC biofilm reactor for 14 d at 37 °C. Upper image: Bar graph of plate count data for adhesion of viable *P. aeruginosa* bacteria to the catheter surfaces. Lower images: Representative fluorescence microscopic images of surface live (green) (A) and/or dead (red) (B) bacteria on different catheters, acquired by oil immersion 60× objective lens, scale bar 20 μm.

caused by *S. epidermidis* alone is estimated to $2 billion annually in US.[65] In contrast, Gram-negative bacteria account for ∼30% of all episodes of nosocomial bacteremia,[66,67] and *P. aeruginosa* is reported to cause 16% of all the CRBSIs.[1,68] Infections caused by *P. aeruginosa* often occur in patients with more serious underlying disease, e.g., extensive trauma.[69] Further, it is important to examine the antimicrobial effect of NO release catheters against this particular strain of bacteria because *P. aeruginosa* possesses the NO reductase enzyme which makes the bacteria cells able to metabolize and deactivate NO, and convert NO to nitrous oxide (N_2O) and ultimately nitrogen.[70,71]

The CDC biofilm reactor used in this study provides a model that offers an environment that mimics the bacterial growth on the polymer surface under moderate fluid sheer stress.[72] Therefore, this methodology was utilized to simulate bacterial biofilm development on the surface of IV catheters that will take place in the bloodstream. All SNAP catheters and control

DOI: 10.1021/acsbiomaterials.6b00622
ACS Biomater. Sci. Eng. 2017, 3, 349−359

catheters were initially sterilized by ethylene oxide (EO) and kept antiseptic before use. Ethylene oxide sterilization is a routine procedure for sterilizing clinical appliances within hospitals, during which the devices are subjected to high temperature and high humidity level.[73,74] The amount of SNAP remaining in the catheters after EO sterilization was determined to be 97.4 ± 0.8%, suggesting that SNAP is very stable as crystals embedded within the CarboSil polymer during the sterilization process. The sterilized SNAP catheter segments and control catheter segments (n = 4) were mounted onto coupons within the CDC bioreactor and bacterial biofilms were formed on the surface of both catheters over a 14 d period at 37 °C. After that time period, the number of live microbes on the surface of the catheters was determined by plate counting as well as fluorescence imaging. As shown in Figures 8 and 9, the number of viable *S. epidermidis* and *P. aeruginosa* adhered on the surface of SNAP impregnated catheter segments after 14 d was reduced by 2.0 and 2.5 log units, respectively. These findings were substantiated by the fluorescence imaging data, in which the control catheter surfaces were covered by a high biomass biofilm while the SNAP catheter surfaces had noticeably less bacterial coverage and most of the bacteria on SNAP catheter surfaces were single bacterial cells. The results demonstrate that decreasing bacteria colonization and biofilm formation on the surfaces of SNAP-impregnated CarboSil catheter through continuous NO release may lead to reduced risk of catheter-related bloodstream infections.

3.7. Reduction of Thrombus Formation in Rabbit Model. In vivo experiments using an acute 7 h rabbit thrombogenicity model were conducted to examine the benefits of the SNAP-impregnated CarboSil IV catheters with respect to decreasing clot formation. One SNAP catheter and one control catheter were placed into the external jugular veins of each rabbit (n = 3) for 7 h. At the end of the 7 h implantation, the catheters were carefully removed from the blood vessel while any thrombus formation was left intact on the catheter surface. In order to determine the area of clot formation, digital images of both the SNAP impregnated and control catheters were taken and the two-dimensional representation of the clot areas were quantitated using ImageJ software from NIH. The clot area on the control catheter was 0.84 ± 0.19 cm^2/catheter, whereas the clot area on the SNAP catheter was 0.03 ± 0.01 cm^2/catheter, considerably less than the controls (see Figure 10).

The NO release rates from the postsurgery SNAP catheters were quantitated using chemiluminescence and the SNAP catheters were shown to maintain NO release at an average flux of 4.4 ± 1.1 × 10^{-10} mol cm^{-2} min^{-1} at 37 °C. This result clearly illustrates that continuous localized NO release from the SNAP impregnated CarboSil catheter has the potential to greatly reduce the risk of clot formation on the catheter's surface, thereby maintaining the functionality of IV catheters during use and reducing the risk of stroke or deep vein thrombosis associated with detached blood clots.

4. CONCLUSION

In summary, a simple solvent impregnation procedure has been adapted to incorporate SNAP into CarboSil 20 80A polymer. The impregnation process was optimized to achieve maximized SNAP loading and long-term NO release. The majority of the SNAP incorporated in 15 wt % SNAP-impregnated CarboSil films exists in its crystalline form, and more than 70% of the total NO release originates directly from the SNAP decomposition within the bulk of the polymer phase. The 15 wt % SNAP-impregnated CarboSil catheters release NO at physiological levels for at least 14 d. The NO release catheters reduce viable *S. epidermidis* and *P. aeruginosa* bacteria adhesion to the surface of the catheters after 14 d was by 2 and 2.5 log units, respectively. The SNAP catheters also exhibit minimal clot formation after 7 h of implantation in a rabbit model when compared to the control CarboSil catheters. Overall, both the in vitro and in vivo studies clearly demonstrate the potential of the SNAP impregnation method to improve the hemocompatibility/antimicrobial activity of IV catheters made with CarboSil polymer. It is anticipated that these results will encourage further pursuit of this strategy in designing the next-generation commercial IV catheters and other implantable biomedical devices to greatly reduce risk of infection and thrombosis in patients.

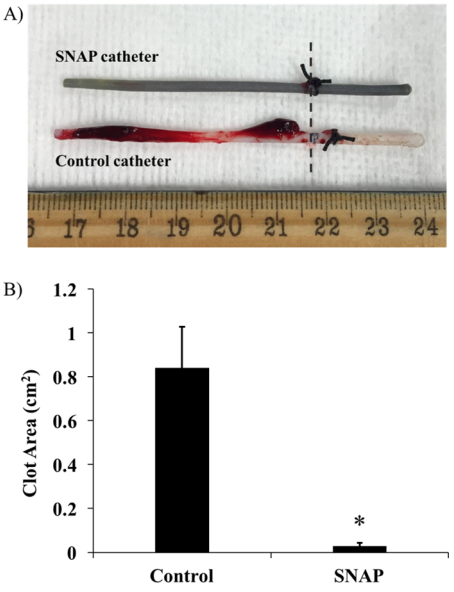

Figure 10. Five centimeters of the catheters (left of the dashed line) were inserted into the rabbit external jugular veins for 7 h. (A) Representative pictures of the thrombus formation on the SNAP-impregnated CarboSil and control CarboSil catheters from one rabbit experiment. (B) Two-dimensional representation of the clot area (cm^2) on SNAP and control catheter in rabbit veins for 7 h, as quantitated using ImageJ software by NIH. Data are mean ± SEM for n = 3 animal experiments. * = $p < 0.05$.

■ ASSOCIATED CONTENT

Supporting Information

The Supporting Information is available free of charge on the ACS Publications website at DOI: 10.1021/acsbiomaterials.6b00622.

Experimental details on the SNAP synthesis protocol, polarized microscope images, powder X-ray diffraction (PXRD) studies, ethylene oxide (EO) sterilization, in vitro 14 day antibiofilm studies, and in vivo 7 h rabbit experiments (PDF)

■ AUTHOR INFORMATION

Corresponding Author

*E-mail: mmeyerho@umich.edu. Telephone: (734) 763-5916.

ORCID

Adam J. Matzger: 0000-0002-4926-2752

DOI: 10.1021/acsbiomaterials.6b00622
ACS Biomater. Sci. Eng. 2017, 3, 349−359

Mark E. Meyerhoff: 0000-0002-7841-281X

Notes

The authors declare no competing financial interest.

■ ACKNOWLEDGMENTS

This work was supported by grants from the National Institutes of Health (HL-128337, DK-100161, and GM-106180). We wish to thank Ms. Judy Poore for the help with the use of Leica 3050S cryostat. We also want to thank DSM company for the gift of the CarboSil 20 80A polymer.

■ REFERENCES

(1) Parameswaran, R.; Sherchan, J. B.; Muralidhar Varma, D.; Mukhopadhyay, C.; Vidyasagar, S. Intravascular catheter-related infections in an Indian tertiary care hospital. *J. Infect. Dev. Countries* **2011**, *5*, 452−458.

(2) Venturini, E.; Becuzzi, L.; Magni, L. Catheter-induced thrombosis of the superior vena cava. *Case Rep. Vasc. Med.* **2012**, *2012*, 469619.

(3) Wu, H.; Moser, C.; Wang, H.-Z.; Høiby, N.; Song, Z.-J. Strategies for combating bacterial biofilm infections. *Int. J. Oral Sci.* **2015**, *7*, 1−7.

(4) Linenberger, M. L. Catheter-related thrombosis: risks, diagnosis, and management. *J. Natl. Compr. Canc. Netw.* **2006**, *4*, 889−901.

(5) Kamphuisen, P. W.; Lee, A. Y. Y. Catheter-related thrombosis: lifeline or a pain in the neck? *Hematology Am. Soc. Hematol. Educ. Program* **2012**, *2012*, 638−644.

(6) Lavery, K. S.; Rhodes, C.; Mcgraw, A.; Eppihimer, M. J. Anti-thrombotic technologies for medical devices. *Adv. Drug Delivery Rev.* **2016**, DOI: 10.1016/j.addr.2016.07.008.

(7) Baskin, J. L.; Pui, C.; Reiss, U.; Wilimas, J. A.; Metzger, M. L.; Ribeiro, R. C.; Howard, S. C. Management of occlusion and thrombosis associated with long-term indwelling central venous catheters. *Lancet* **2009**, *374*, 159−169.

(8) Lee, T.; Lok, C.; Vazquez, M.; Moist, L.; Maya, I.; Mokrzycki, M. Minimizing hemodialysis catheter dysfunction: an ounce of prevention. *Int. J. Nephrol.* **2012**, *2012*, 1.

(9) Abad, C.; Safdar, N. Catheter-related bloodstream infections. *Infect. Dis. Spec. Ed.* **2011**.

(10) Fletcher, S. Catheter-related bloodstream infection. *Contin. Educ. Anaesthesia, Crit. Care Pain* **2005**, *5*, 49−51.

(11) Donlan, R. M. Biofilm elimination on intravascular catheters: Important considerations for the infectious disease practitioner. *Clin. Infect. Dis.* **2011**, *52*, 1038−1045.

(12) Donlan, R. M. Biofilm formation: a clinically relevant microbiological process. *Clin. Infect. Dis.* **2001**, *33*, 1387−1392.

(13) Hoiby, N.; Ciofu, O.; Johansen, H. K.; Song, Z.; Moser, C.; Jensen, P. O.; Molin, S.; Givskov, M.; Tolker-Nielsen, T.; Bjarnsholt, T. The clinical impact of bacterial biofilms. *Int. J. Oral Sci.* **2011**, *3*, 55−65.

(14) Hengzhuang, W.; Wu, H.; Ciofu, O.; Song, Z.; Høiby, N. In vivo pharmacokinetics/pharmacodynamics of colistin and imipenem in pseudomonas aeruginosa biofilm infection. *Antimicrob. Agents Chemother.* **2012**, *56*, 2683−2690.

(15) Mermel, L. A.; Allon, M.; Bouza, E.; Craven, D. E.; Flynn, P.; O'Grady, N. P.; Raad, I. I.; Rijnders, B. J.; Sherertz, R. J.; Warren, D. K. Clinical practice guidelines for the diagnosis and management of intravascular catheter-related infection: 2009 Update by the Infectious Diseases Society of America. *Clin. Infect. Dis.* **2009**, *49*, 1−45.

(16) Kiedrowski, M. R.; Horswill, A. R. New approaches for treating staphylococcal biofilm infections. *Ann. N. Y. Acad. Sci.* **2011**, *1241*, 104−121.

(17) O'Grady, N. P.; Alexander, M.; Dellinger, E. P.; Gerberding, J. L.; Heard, S. O.; Maki, D. G.; Masur, H.; McCormick, R. D.; Mermel, L. A.; Pearson, M. L.; et al. Guidelines for the prevention of intravascular catheter-related infections. *Morbidity and Mortality Weekly Report* **2002**, *51* (RR10), 1−26.

(18) Warren, D. K.; Quadir, W. W.; Hollenbeak, C. S.; Elward, A. M.; Cox, M. J.; Fraser, V. J. Attributable cost of catheter-associated bloodstream infections among intensive care patients in a nonteaching hospital. *Crit. Care Med.* **2006**, *34*, 2084−2089.

(19) Diekema, D. J.; Beekmann, S. E.; Chapin, K. C.; Morel, K. A.; Munson, E.; Doern, G. V. Epidemiology and outcome of nosocomial and community-onset bloodstream infection. *J. Clin. Microbiol.* **2003**, *41*, 3655−3660.

(20) Rosenthal, V. D.; Guzman, S.; Orellano, P. W. Nosocomial infections in medical-surgical intensive care units in Argentina: attributable mortality and length of stay. *Am. J. Infect. Control* **2003**, *31*, 291−295.

(21) Filippi, L.; Pezzati, M.; Di Amario, S.; Poggi, C.; Pecile, P. Fusidic acid and heparin lock solution for the prevention of catheter-related bloodstream infections in critically ill neonates: a retrospective study and a prospective, randomized trial. *Pediatr. Crit. Care Med.* **2007**, *8*, 556−562.

(22) Smith, S.; Dawson, S.; Hennessey, R.; Andrew, M. Maintenance of the patency of indwelling central venous catheters: is heparin necessary? *J. Pediatr. Hematol./Oncol.* **1991**, *13*, 141−143.

(23) Stephens, L. C.; Haire, W. D.; Tarantolo, S.; Reed, E.; Schmit-Pokorny, K.; Kessinger, A.; Klein, R. Normal saline versus heparin flush for maintaining central venous catheter patency during apheresis collection of peripheral blood stem cells (PBSC). *Transfus. Sci.* **1997**, *18*, 187−193.

(24) Dogra, G. K.; Herson, H.; Hutchison, B.; Irish, A. B.; Heath, C. H.; Golledge, C.; Luxton, G.; Moody, H. Prevention of tunneled hemodialysis catheter-related infections using catheter-restricted filling with gentamicin and citrate: a randomized controlled study. *J. Am. Soc. Nephrol.* **2002**, *13*, 2133−2139.

(25) Yahav, D.; Rozen-Zvi, B.; Gafter-Gvili, A.; Leibovici, L.; Gafter, U.; Paul, M. Antimicrobial lock solutions for the prevention of infections associated with intravascular catheters in patients undergoing hemodialysis: systematic review and meta-analysis of randomized, controlled trials. *Clin. Infect. Dis.* **2008**, *47*, 83−93.

(26) Vaughn, M.; Kuo, L.; Liao, J. Estimation of nitric oxide production and reaction rates in tissue by use of a mathematical model. *Am. J. Physiol.* **1998**, *274*, 2163−2176.

(27) Wo, Y.; Brisbois, E. J.; Bartlett, R. H.; Meyerhoff, M. E. Recent advances in thromboresistant and antimicrobial polymers for biomedical applications: just say yes to nitric oxide (NO). *Biomater. Sci.* **2016**, *4*, 1161−1183.

(28) Wang, Y.; Chen, S.; Pan, Y.; Gao, J.; Tang, D.; Kong, D.; Wang, S. Rapid in situ endothelialization of small diameter vascular graft with catalytic nitric oxide generation and promoted endothelial cell adhesion. *J. Mater. Chem. B* **2015**, *3*, 9212−9222.

(29) Carpenter, A. W.; Schoenfisch, M. H. Nitric oxide release: part II. Therapeutic applications. *Chem. Soc. Rev.* **2012**, *41*, 3742−3752.

(30) Zhou, X.; Zhang, J.; Feng, G.; Shen, J.; Kong, D.; Zhao, Q. Nitric oxide-releasing biomaterials for biomedical applications. *Curr. Med. Chem.* **2016**, *23*, 2579−2601.

(31) Loscalzo, J. Nitric oxide insufficiency, platelet activation, and arterial thrombosis. *Circ. Res.* **2001**, *88*, 756−762.

(32) Yoo, J.-W.; Nurhasni, H.; Cao, J.; Choi, M.; Kim, I.; Lee, B. L.; Jung, Y. Nitric oxide-releasing poly(lactic-co-glycolic acid)- polyethylenimine nanoparticles for prolonged nitric oxide release, antibacterial efficacy, and in vivo wound healing activity. *Int. J. Nanomed.* **2015**, *10*, 3065−3080.

(33) Ghaffari, A.; Miller, C. C.; McMullin, B.; Ghahary, A. Potential application of gaseous nitric oxide as a topical antimicrobial agent. *Nitric Oxide* **2006**, *14*, 21−29.

(34) Arora, D. P.; Hossain, S.; Xu, Y.; Boon, E. M. Nitric oxide regulation of bacterial biofilms. *Biochemistry* **2015**, *54*, 3717−3728.

(35) McMullin, B. B.; Chittock, D. R.; Roscoe, D. L.; Garcha, H.; Wang, L.; Miller, C. C. The antimicrobial effect of nitric oxide on the bacteria that cause nosocomial pneumonia in mechanically ventilated patients in the intensive care unit. *Respir. Care* **2005**, *50*, 1451−1456.

(36) Plate, L.; Marletta, M. A. Nitric oxide modulates bacterial biofilm formation through a multi-component cyclic-di-GMP signaling network. *Mol. Cell* **2012**, *46*, 449−460.

DOI: 10.1021/acsbiomaterials.6b00622
ACS Biomater. Sci. Eng. 2017, 3, 349−359

(37) Barraud, N.; Kelso, M. J.; Rice, S. A.; Kjelleberg, S. Nitric oxide: a key mediator of biofilm dispersal with applications in infectious diseases. *Curr. Pharm. Des.* **2015**, *21*, 31−42.
(38) Brisbois, E. J.; Handa, H.; Meyerhoff, M. E. Recent advances in hemocompatible polymers for biomedical applications. In *Advanced Polymers in Medicine*; Puoci, F., Ed.; Springer International: Cham, Switzerland, 2015; pp 481−511.
(39) Riccio, D. A.; Schoenfisch, M. H. Nitric oxide release: part I. macromolecular scaffolds. *Chem. Soc. Rev.* **2012**, *41*, 3731−3741.
(40) Jen, M. C.; Serrano, M. C.; van Lith, R.; Ameer, G. A. Polymer-based nitric oxide therapies: recent insights for biomedical applications. *Adv. Funct. Mater.* **2012**, *22*, 239−260.
(41) Qiao, S.; Cabello, C. M.; Lamore, S. D.; Lesson, J. L.; Wondrak, G. T. D-Penicillamine targets metastatic melanoma cells with induction of the unfolded protein response (UPR) and Noxa (PMAIP1)-dependent mitochondrial apoptosis. *Apoptosis* **2012**, *17*, 1079−1094.
(42) Brisbois, E. J.; Handa, H.; Major, T. C.; Bartlett, R. H.; Meyerhoff, M. E. Long-term nitric oxide release and elevated temperature stability with S-nitroso-N-acetylpenicillamine (SNAP)-doped Elast-eon E2As polymer. *Biomaterials* **2013**, *34*, 6957−6966.
(43) Wo, Y.; Li, Z.; Brisbois, E. J.; Colletta, A.; Wu, J.; Major, T. C.; Xi, C.; Bartlett, R. H.; Matzger, A. J.; Meyerhoff, M. E. Origin of long-term storage stability and nitric oxide release behavior of CarboSil polymer doped with *S*-nitroso-*N*-acetyl-d-penicillamine. *ACS Appl. Mater. Interfaces* **2015**, *7*, 22218−22227.
(44) Colletta, A.; Wu, J.; Wo, Y.; Kappler, M.; Chen, H.; Xi, C.; Meyerhoff, M. E. *S*-Nitroso-*N*-acetylpenicillamine (SNAP) impregnated silicone foley catheters: a potential biomaterial/device to prevent catheter-associated urinary tract infections. *ACS Biomater. Sci. Eng.* **2015**, *1*, 416−424.
(45) Brisbois, E. J.; Major, T. C.; Goudie, M. J.; Bartlett, R. H.; Meyerhoff, M. E.; Handa, H. Improved hemocompatibility of silicone rubber extracorporeal tubing via solvent swelling-impregnation of S-nitroso-N-acetylpenicillamine (SNAP) and evaluation in rabbit thrombogenicity model. *Acta Biomater.* **2016**, *37*, 111−119.
(46) Clarke, M. L.; Wang, J.; Chen, Z. Conformational changes of fibrinogen after adsorption. *J. Phys. Chem. B* **2005**, *109*, 22027−22035.
(47) Handa, H.; Major, T. C.; Brisbois, E. J.; Amoako, K. A.; Meyerhoff, M. E.; Bartlett, R. H. Hemocompatibility comparison of biomedical grade polymers using rabbit thrombogenicity model for preparing nonthrombogenic nitric oxide releasing surfaces. *J. Mater. Chem. B* **2014**, *2*, 1059−1067.
(48) Lee, J. N.; Park, C.; Whitesides, G. M. Solvent compatibility of poly(dimethylsiloxane)-based microfluidic devices. *Anal. Chem.* **2003**, *75*, 6544−6554.
(49) Xu, L. C.; Siedlecki, C. a. Submicron-textured biomaterial surface reduces staphylococcal bacterial adhesion and biofilm formation. *Acta Biomater.* **2012**, *8*, 72−81.
(50) Otto, M. Staphylococcus epidermidis—the'accidental'pathogen. *Nat. Rev. Microbiol.* **2009**, *7*, 555−567.
(51) Szacilowski, K.; Stasicka, Z. S-Nitrosothiols: materials, reactivity and mechanisms. *Prog. React. Kinet. Mech.* **2001**, *26*, 1−58.
(52) Shishido, S. M.; Oliveira, M. G. Polyethylene glycol matrix reduces the rates of photochemical and thermal release of nitric oxide from S-nitroso-N-acetylcysteine. *Photochem. Photobiol.* **2000**, *71*, 273−280.
(53) Graeme, K. A.; Pollack, C. V. Heavy metal toxicity, part I: arsenic and mercury. *Journal of Emergency Medicine* **1998**, *16*, 45−56.
(54) Jones, M. M.; Weaver, A. D.; Weller, W. L. The relative effectiveness of some chelating agents as antidotes in acute cadmium poisoning. *Res. Commun. Chem. Pathol. Pharmacol.* **1978**, *22*, 581−588.
(55) Helms, C.; Kim-Shapiro, D. B. Hemoglobin-mediated nitric oxide signaling. *Free Radical Biol. Med.* **2013**, *61*, 464−472.
(56) Donadee, C.; Raat, N. J. H.; Kanias, T.; Tejero, J.; Lee, J. S.; Kelley, E. E.; Zhao, X.; Liu, C.; Reynolds, H.; Azarov, I.; et al. Nitric oxide scavenging by red cell microparticles and cell free hemoglobin as a mechanism for the red cell storage lesion. *Circulation* **2011**, *124*, 465−476.
(57) Ziebuhr, W.; Hennig, S.; Eckart, M.; Kränzler, H.; Batzilla, C.; Kozitskaya, S. Nosocomial infections by Staphylococcus epidermidis: how a commensal bacterium turns into a pathogen. *Int. J. Antimicrob. Agents* **2006**, *28* (Suppl 1), S14−S20.
(58) Zhang, L.; Morrison, M.; Ó Cuív, P.; Evans, P.; Rickard, C. M. Genome sequence of Staphylococcus epidermidis strain AU12-03, isolated from an intravascular catheter. *J. Bacteriol.* **2012**, *194*, 6639.
(59) Hall-stoodley, L.; Costerton, J. W.; Stoodley, P. Bacterial biofilms: from the natural environment to infectious diseases. *Nat. Rev. Microbiol.* **2004**, *2*, 95−108.
(60) Mack, D.; Davies, A. P.; Harris, L. G.; Jeeves, R.; Pascoe, B.; Knobloch, J. K.; Rohde, H.; Wilkinson, T. S. *Biomaterials Associated Infection*; Moriarty, T. F., Zaat, S. A. J., Busscher, H. J., Eds.; Springer: New York, 2013.
(61) Fey, P. D.; Olson, M. E. Current concepts in biofilm formation of Staphylococcus epidermidis. *Future Microbiol.* **2010**, *5*, 917−933.
(62) Svensson, E.; Hanberger, H.; Nilsson, M.; Nilsson, L. E. Factors affecting development of rifampicin resistance in biofilm- producing Staphylococcus epidermidis. *J. Antimicrob. Chemother.* **1997**, *39*, 817−820.
(63) Nakajima, J.; Hitomi, S.; Koganemaru, H.; Nakai, Y. Isolation of Staphylococcus epidermidis intermediately resistant to vancomycin in a case of central venous catheter-associated bloodstream infection. *J. Infect. Chemother.* **2013**, *19*, 983−986.
(64) Cabrera-Contreras, R.; Morelos-Ramírez, R.; Galicia-Camacho, A. N.; Meléndez-Herrada, E. Antibiotic resistance and biofilm production in Staphylococcus epidermidis strains, isolated from a tertiary care hospital in Mexico City. *ISRN Microbiol.* **2013**, *2013*, 1−5.
(65) Costerton, J. W.; Stewart, P. S.; Greenberg, E. P. Bacterial biofilms: a common cause of persistent infections. *Science* **1999**, *284*, 1318−1322.
(66) Dunn, D. L. Diagnosis and treatment of infection. In *Surgery: Basic Science and Clinical Evidence*; Norton, J. A., Barie, P. S., Bollinger, R. R., Chang, A. E., Lowry, S. F., Mulvihill, S. J., Pass, H. I., Thompson, R. W., Eds.; Springer: New York, 2008; pp 209−235.
(67) Sligl, W. I.; Dragan, T.; Smith, S. W. Nosocomial gram-negative bacteremia in intensive care: epidemiology, antimicrobial susceptibilities, and outcomes. *Int. J. Infect. Dis.* **2015**, *37*, 129−134.
(68) Gahlot, R.; Nigam, C.; Kumar, V.; Yadav, G.; Anupurba, S. Catheter-related bloodstream infections. *Int. J. Crit. Illn. Inj. Sci.* **2014**, *4*, 162−167.
(69) Dunn, D. L. Gram-negative bacterial sepsis and sepsis syndrome. *Surg. Clin. North Am.* **1994**, *74*, 621−635.
(70) Reighard, K. P.; Schoenfisch, M. H. Antibacterial action of nitric oxide-releasing chitosan oligosaccharides against Pseudomonas aeruginosa under aerobic and anaerobic conditions. *Antimicrob. Agents Chemother.* **2015**, *59*, 6506−6513.
(71) Carpenter, A. W.; Slomberg, D. L.; Rao, K. S.; Schoenfisch, M. H. Influence of scaffold size on bactericidal activity of nitric oxide-releasing silica nanoparticles. *ACS Nano* **2011**, *5*, 7235−7244.
(72) Goeres, D. M.; Loetterle, L. R.; Hamilton, M. A.; Murga, R.; Kirby, D. W.; Donlan, R. M. Statistical assessment of a laboratory method for growing biofilms. *Microbiology* **2005**, *151*, 757−762.
(73) Mendes, G. C.; Brandão, T. R.; Silva, C. L. Ethylene oxide sterilization of medical devices: a review. *Am. J. Infect. Control* **2007**, *35*, 574−581.
(74) Matthews, I. P.; Gibson, C.; Samuel, A. H. Sterilisation of implantable devices. *Clin. Mater.* **1994**, *15*, 191−215.

DOI: 10.1021/acsbiomaterials.6b00622
ACS Biomater. Sci. Eng. 2017, 3, 349−359